STRUCTURAL ANALYSIS OF A CLAW COUPLING

Dănuţ Zahariea[1]

[1] "Gheorghe Asachi" Technical University of Iasi-Romania,
Department of Fluid Mechanics, Hydraulic Machines and Drives
Blvd. D. Mangeron, No. 59A, 700050, Iasi, Romania

Corresponding author: Dănuţ Zahariea, e-mail: dzahariea@tuiasi.ro

Abstract: In this paper the displacements, as well as the von Misses stresses of the claw coupling will be analyzed using CATIA Generative Structural Analysis workbench. Several constructive types will be analyzed: the coupling with one claw with and without cylindrical pin, as well as the coupling with three claws. The structural analysis procedure will be presented: creating the 3D model, configuring the mesh, applying the restraints, applying the loads, applying the interaction conditions, running the numerical analysis and results visualization. The visual representation of the numerical results will be analyzed at both the assembly level and the part level. The assembly level analysis allows identifying the most critical section of the entire coupling. The part level analysis allows observing the results for every component of the claw coupling.
Key words: claw coupling, structural analysis, CATIA.

1. INTRODUCTION

In order to obtain the transmission of the rotation movement and torque between shafts, a coupling can be used. For any type of coupling the geometric characteristics can be obtain by a preliminary calculation using the well known relationship (Drăghici et al., 1978). Thus, the coupling will be checked according with the safety range of the torsional and shearing strengts. Even if, as a result of this preliminary calculation, the coupling is well designed, some additional questions must be solved: which is the stress distribution on each coupling element?; which is the critical section distribution on each coupling element?; there are zones with stress concentration? Unfortunatelly, the preliminary calculation cannot answer to these questions, the problem should be further investigated using advanced numerical methods (3D FEA based investigation). In (Zahariea & Tudorache 2010) the sleeve rigid coupling with cylindrical pins has been investigated using the 3D finite element analysis. This paper is devoted to a 3D finite element analysis based investigation using the CATIA Generative Structural Analysis workbench (Zamani, 2005 and Ghionea, 2007) of the claw coupling. Three different types of claw couplings will be investigated: the coupling with one claw without cylindrical pin (figure 1); the coupling with one claw with cylindrical pin (figure 2) and the coupling with three claws (figure 3).

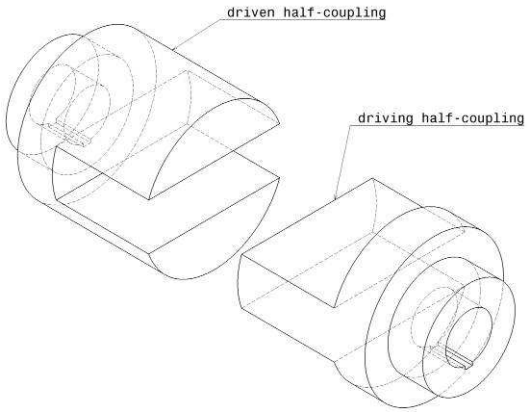

Fig. 1. One claw coupling without cylindrical pin

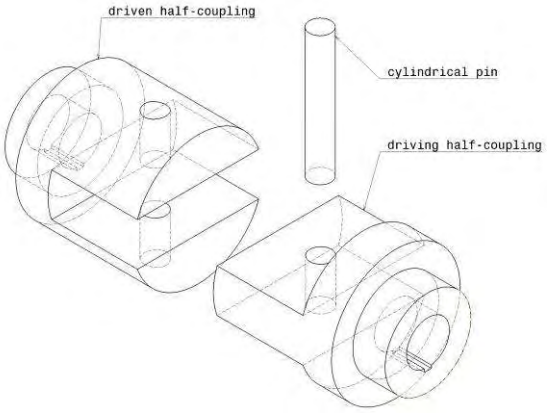

Fig. 2. One claw coupling with cylindrical pin

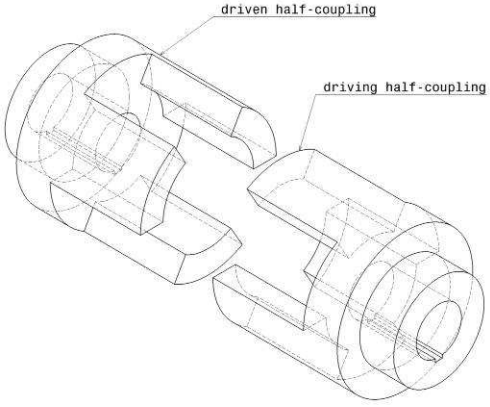

Fig. 3. Three claws coupling

All these three types of claw couplings must ensure the transmission of a mechanical power P=1 kW at the rotation speed of n=500 rpm. Knowing the angular rate $\omega=2\pi n/60=52.3599$ rad/s, the torque $M=P/\omega=19.0986$ Nm and the safety coefficient $k_M=2.0944$, the safety torque can be calculated using the relationship $M_s=k_M M$, the value $M_s=40$ Nm being thus obtained.

The material used for all couplings elements is steel with yield strength $\sigma_{02}=2.5\cdot10^8$ N/m^2.

The global geometric characteristics of the couplings have been obtained using the recommended specifications (Muhs et al, 2008). These global geometric characteristics of the couplings can be observed in figures 4, 5 and 6.

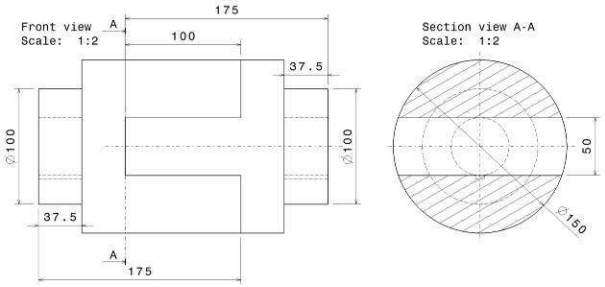

Fig. 4. One claw coupling without cylindrical pin. Geometric characteristics

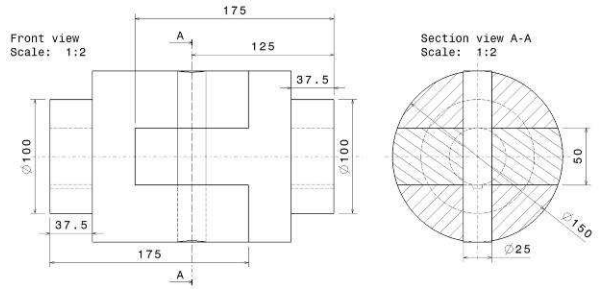

Fig. 5. One claw coupling with cylindrical pin. Geometric characteristics

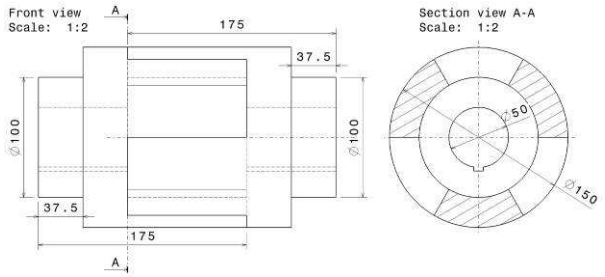

Fig. 6. Three claws coupling. Geometric characteristics

The structural analysis will be developed according to a procedure which the main steps are: creating the 3D model; creating the 3D finite element model; applying the restraints and the loads; applying the interaction conditions between all the coupling elements; running the numerical analysis and the results visualization. As for the results, the graphic representation of the von Misses stress distribution, the displacements and the deformed mesh will be analysed. Also, a comparative study of the influence of the mesh type on the global error rate will be presented. Further investigations should be made on all these three types of claw couplings including also the two shafts (the driving and the driven shafts), as well as the two keys which made the connection between the shafts and the half-couplings.

2. ONE CLAW COUPLING WITHOUT PIN

2.1. The finite element model

In order to obtain the finite element model the tetrahedral elements will be used of both types: linear and parabolic. For the same 3D model, different finite element models can be obtained changing the characteristic parameters: the size and the sag. There are several methods used to change the mesh parameters: the global method; the local method and the adaptive method. In order to select the best finite element model the global error rate criterion ($\varepsilon_{cr}\approx10\%$) will be used.

Using the global method with the following values: size=15mm and sag=3 mm, for the mesh obtained with linear finite elements (2287 nodes and 9230 elements) the global error rate is $\varepsilon_l=40.47\%$ and for the mesh obtained with parabolic finite elements (10459 nodes and 10026 elements) the global error rate is $\varepsilon_p=14.79\%$. The deformed mesh is presented in figure 7.

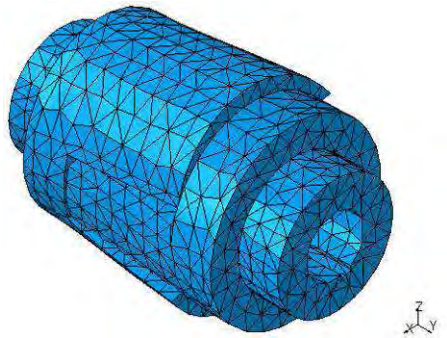

Fig. 7. The deformed mesh by global method

In order to achieve the global error rate imposed, the mesh must be improved. The adaptive method has been used with an objective global error rate of 11%. The improved mesh obtained with parabolic finite elements (41088 nodes and 29725 elements) allows the obtaining of a global error rate of 10.11% that is very close to the imposed criterion value. The improved deformed mesh is presented in figure 8.

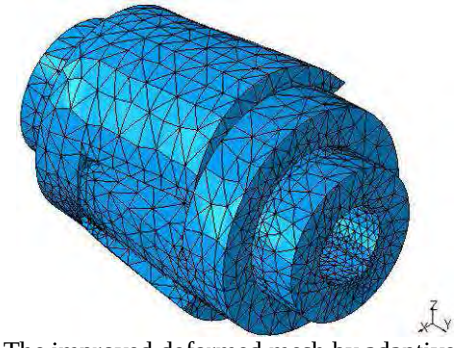

Fig. 8. The improved deformed mesh by adaptive method

2.2. The restraints, the loads and the interaction condition

On the driving half-coupling a pivot restraint has been applied. On the driven half-coupling a user-defined restraint blocking the x-axis translation and the y-axis rotation has been applied. The moment M_s has been applied on driving half-coupling. The contact connection property has been used between the corresponding surfaces on both driving and driven half-couplings. In figure 9 the 3D model with restraints, loads and interaction condition is presented.

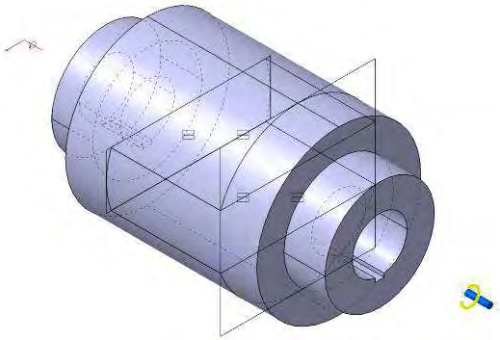

Fig. 9. The restraints, the loads and the interaction conditions

2.3. The analysis results

The displacements for both elements of the one claw coupling are presented in figure 10. The von Misses stresses for one claw coupling are presented in figure 11. The von Misses stresses for the driven half-coupling are presented in figure 12. The von Misses stresses for the driving half-coupling are presented in figure 13.

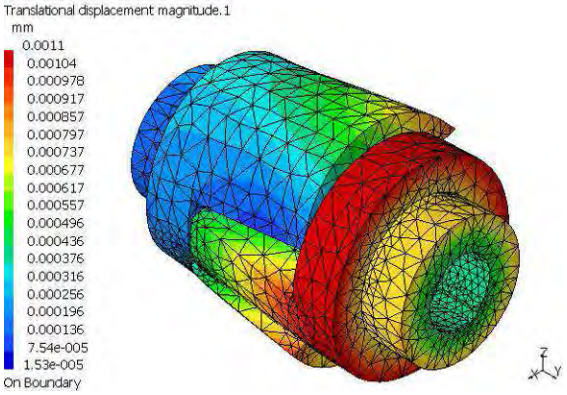

Fig. 10. The displacements

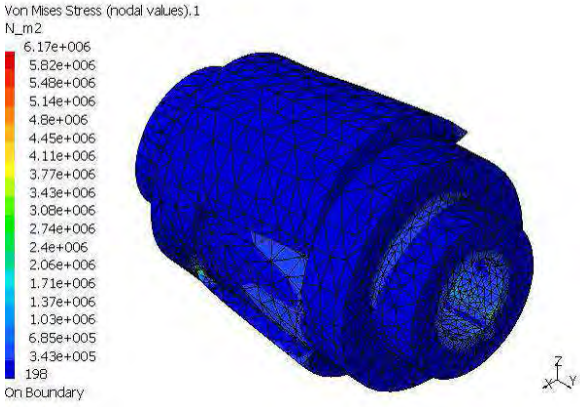

Fig. 11. The von Mises stress for one claw coupling

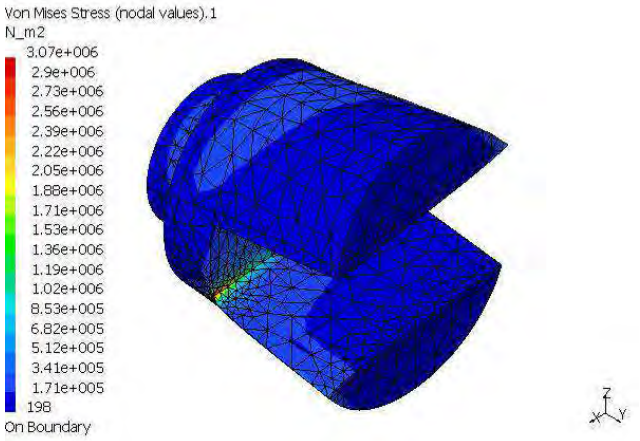

Fig. 12. The von Mises stress for the driven half-coupling.

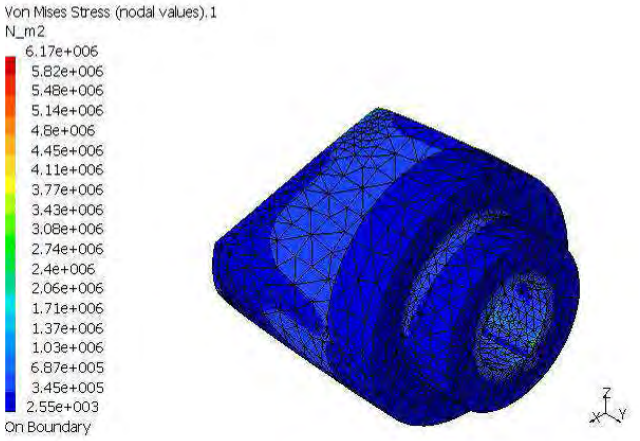

Fig. 13. The von Mises stress for the driving half-coupling

3. ONE CLAW COUPLING WITH PIN

3.1. The finite element model

The same level of the global error rate (ε≈10%) for selecting the best finite element model has been used. Using the global method with the following values: size=15mm and sag=3 mm, for the mesh obtained with linear finite elements (2605 nodes and 10360 elements) the global error rate is ε_l=40.84% and for the mesh obtained with parabolic finite elements (16711 nodes and 11797 elements) the global error rate is ε_p=15.75%. The deformed mesh is presented in figure 14.

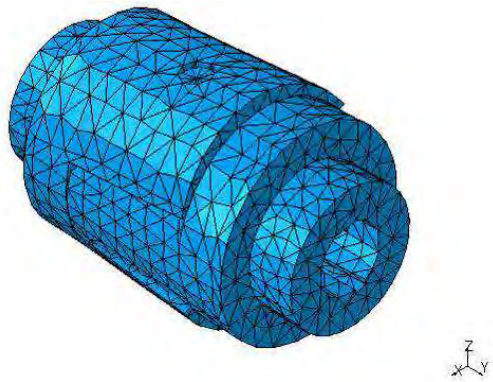

Fig. 14. The deformed mesh by global method

In order to achieve the global error rate imposed, the mesh must be improved. The adaptive method has

been used with an objective global error rate of 11%. The improved mesh obtained with parabolic finite elements (46632 nodes and 33346 elements) allows the obtaining of a global error rate of 10.73% that is very close to the imposed criterion value. The improved deformed mesh is presented in figure 15.

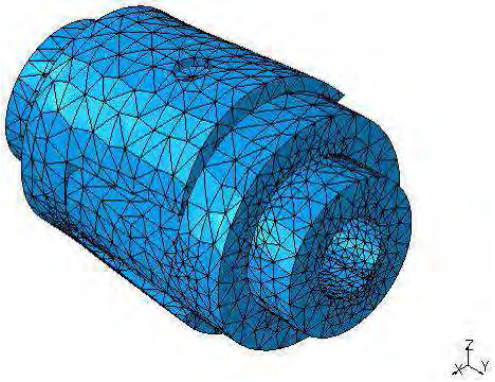

Fig. 15. The improved deformed mesh by adaptive method

3.2. The restraints, the loads and the interaction condition

On the driving half-coupling a pivot restraint has been applied. On the driven half-coupling a user-defined restraint blocking the y-axis rotation has been applied. On the cylindrical pin a user-defined restraint blocking the z-axis translation and rotation has been applied. The moment M_s has been applied on driving half-coupling. The contact connection property has been used between the corresponding surfaces on both driving and driven half-couplings, as well as on the cylindrical pin. In figure 16 the 3D model with restraints, loads and interaction condition is presented.

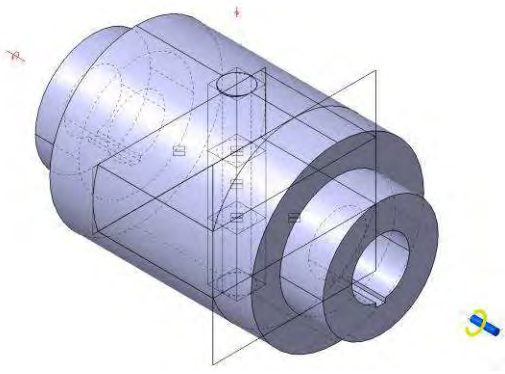

Fig. 16. The restraints, the loads and the interaction conditions.

3.3. The analysis results

The displacements for all elements of the one claw coupling with cylindrical pin are presented in figure 17. The displacements only for the driven half-coupling are presented in figure 18. The displacements only for the driving half-coupling are presented in figure 19. The displacements only for the cylindrical pin are presented in figure 20. The von Misses stresses for one claw coupling with cylindrical pin are presented in figure 21.

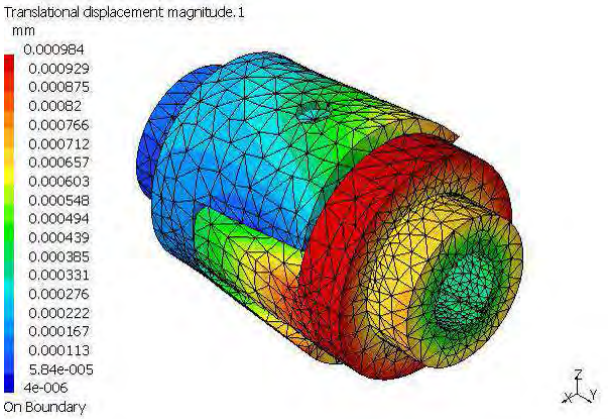

Fig. 17. The displacements of one claw coupling with pin

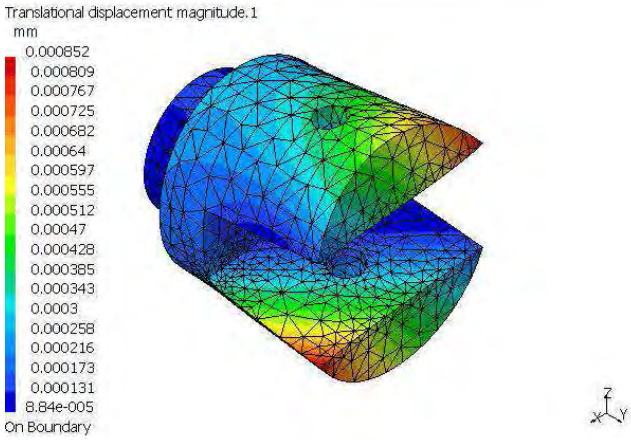

Fig. 18. The displacements for the driven half-coupling

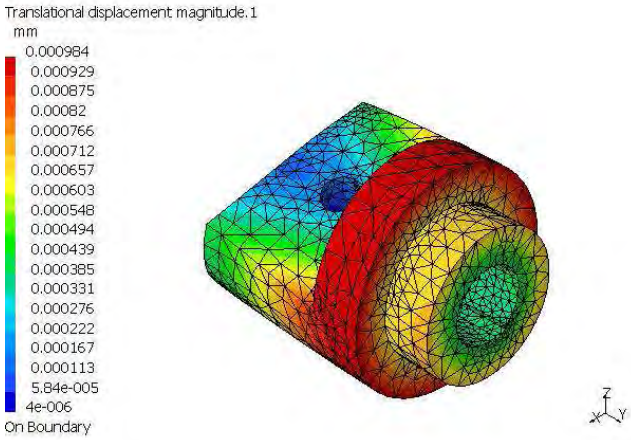

Fig. 19. The displacements for the driving half-coupling

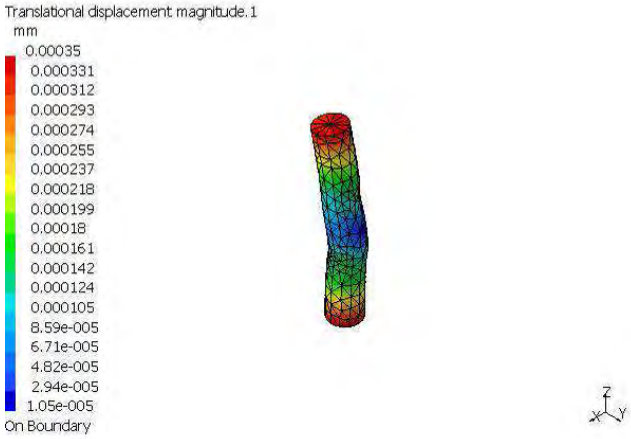

Fig. 20. The displacements for the cylindrical pin

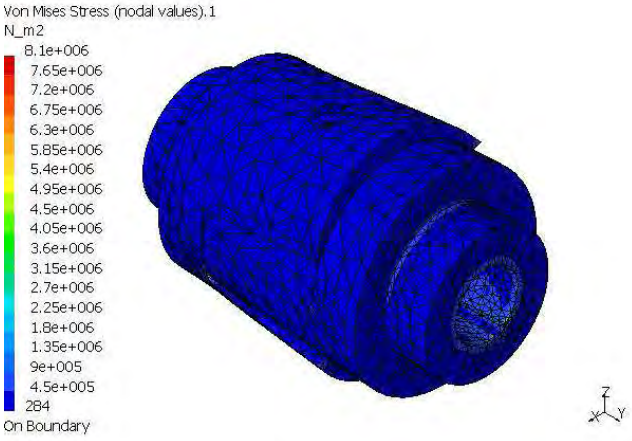

Fig. 21. The von Mises stress for one claw coupling with pin

4. THREE CLAWS COUPLING

4.1. The finite element model

The same level of the global error rate (ε≈10%) for selecting the best finite element model has been used. Using the global method with the following values: size=15mm and sag=3 mm, for the mesh obtained with linear finite elements (2156 nodes and 7963 elements) the global error rate is ε_l=45.29% and for the mesh obtained with parabolic finite elements (13513 nodes and 8657 elements) the global error rate is ε_p=17.031%. The deformed mesh is presented in figure 22.

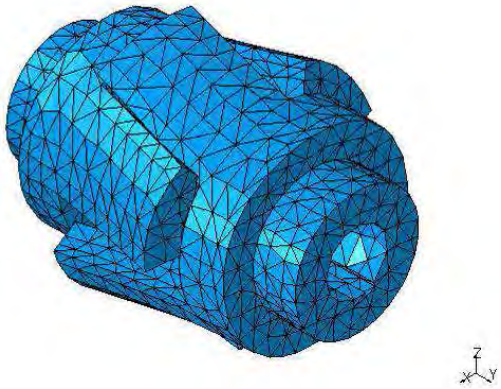

Fig. 22. The deformed mesh by global method

In order to achieve the global error rate imposed, the mesh must be improved. The adaptive method has been used twice: first with an objective global error rate of 12% and second with an objective global error rate of 11%. After the first mesh refinement the improved mesh obtained with parabolic finite elements (36706 nodes and 24732 elements) allows the obtaining of a global error rate of 11.064%. After the second mesh refinement the improved mesh obtained with parabolic finite elements (73599 nodes and 50365 elements) allows the obtaining of a global error rate of 8.74%. The improved deformed mesh obtained after the first stage is presented in figure 23 and the improved deformed mesh obtained after the second stage is presented in figure 24.

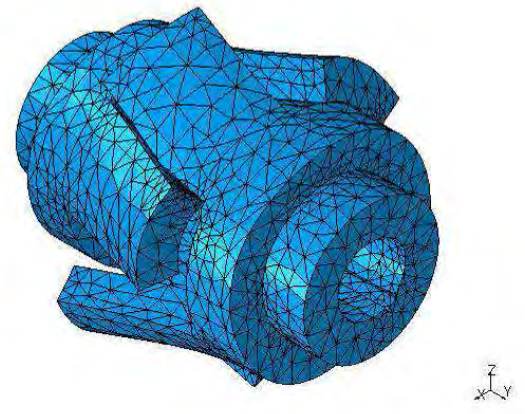

Fig. 23. The improved deformed mesh after the first adaptive stage

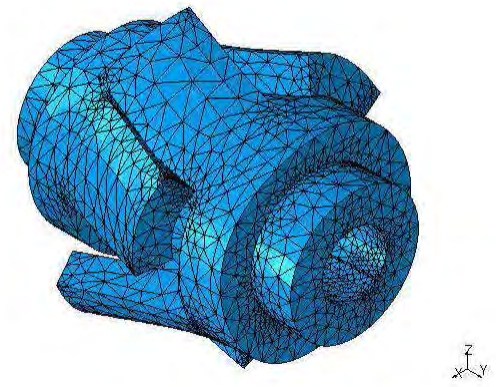

Fig. 24. The improved deformed mesh after the second adaptive stage

4.2. The restraints, the loads and the interaction condition

On the driving half-coupling a pivot restraint has been applied. On the driven half-coupling a user-defined restraint blocking the y-axis rotation has been applied. The moment M_s has been applied on driving half-coupling. The contact connection property has been used between the corresponding surfaces on both driving and driven half-couplings. In figure 25 the 3D model with restraints, loads and interaction condition is presented.

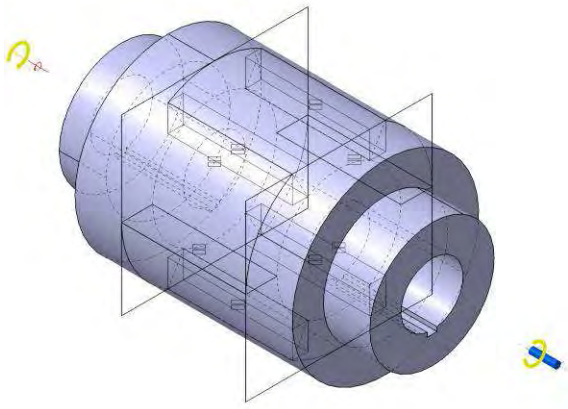

Fig. 25. The restraints, the loads and the interaction conditions

4.3. The analysis results

The displacements for all elements of the three claw coupling are presented in figure 26. The von Misses stresses for the three claws coupling pin are presented in figure 27.

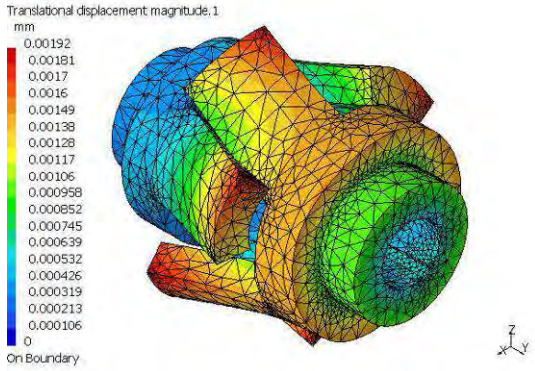

Fig. 26. The displacements of the three claws coupling

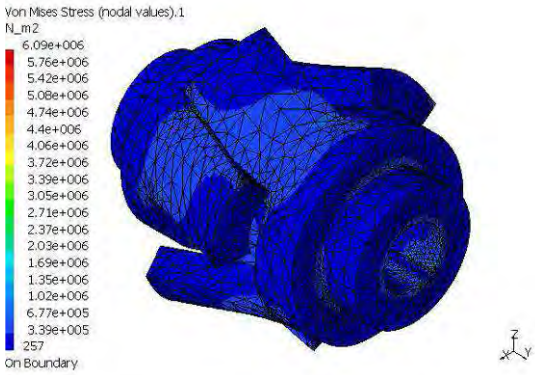

Fig. 27. The von Mises stress for the three claws coupling

5. CONCLUSIONS

The mesh parameters (the geometric parameters: size and sag, and the finite element type: linear or parabolic) have a great influence on the numerical analysis precision. For all the discretized 3D models with linear finite elements the global errors are >40%, which is an unacceptable error level. The linear finite element mesh could be improved by reducing the values of the size and sag parameters. Even if the adaptive mesh modifying method will be used, in order to decrease the global error it will be necessary to increase the number of mesh nodes and elements at very high levels. A better solution can be obtained if the parabolic finite element will be used. For the start global parameters, for all the discretized 3D models with parabolic finite elements the global errors are in range 14%…18%, that is more closely of the desired error level (≈10%). The adaptive method for improving the mesh has been used for all three couplings analysed. For both types of one claw couplings the adaptive mesh refinement has been performed in only one stage, from 14.79% to 10.11% for the case without pin, and from 15.75% to 10.73% for the case with pin. For the last coupling analyzed, two mesh refinement stages have been performed from 17.031% to 11.064% in stage one, and from 11.064% to 8.74% in stage two. The computing time has been increased from 1-2 minutes (starting mesh with linear finite elements) to more than 30 minutes (improved mesh with parabolic finite elements). All computations have been performed on an AMD Athlon 64X2 Dual 3800+ at 2GHz processor with 2 GB RAM and 140 GB HDD. Decreasing the global error objective under 10% or decreasing the mesh parameters size and sag under certain levels can produce more often the computer freeze than the completed analysis.

All figures representing the displacements and the von Misses stress have an amplification magnitude of 30000. The reality corresponds with an amplification magnitude of 1, but for better observations and conclusions it is necessary to increase this parameter.

For all couplings, the critical sections are placed on the claws bases (figures 12, 21 and 27). Some deformations can be observed for all elements: driven half-coupling, driving half-coupling, pin (figures 10, 18, 19, 20 and 26). The area around the holes in both driven and driving half-coupling are stress concentration zone (for the coupling with pin).

An important conclusion has been made observing the animation of the discretized model deformation. During the deformation, the force between claws will change the direction from the tangential direction at the beginning at a certain direction, depending on the torsional moment applied. Thus, the force will have a longitudinal component which will increase the distance from the two half-couplings (assumed to be zero at the beginning) and will be transmited to the shafts. The intensity of this process is decreased for the claw coupling with pin, as the pin will take a significant part of this longitudinal force.

6. REFERENCES

1. Drăghici, I., Achiriloaie, I., Chişu, E., Rădulescu, C.D., Prodan, Gh. (1978). *Calculul şi construcţia cuplajelor*, Tehnica Publishing House, Bucharest.

2. Ghionea, I.G. (2007). *Proiectare asistată în CATIA V5-Elemente teoretice şi aplicaţii*, BREN Publishing House, ISBN 978-973-648-654-8, Bucharest.

3. Muhs, D., Wittel, H., Jannasch, D., Vossiek, J. (2008). *Roloff/Matek-Organe de maşini-Normare, calcul, proiectare-Vol. I, II*, MATRIX ROM Publishing House, ISBN 978-973-755-412-3, Bucharest.

4. Zahariea, D., Tudorache, M. (2010). *Structural Analysis of a Sleeve Rigid Coupling with Cylindrical Pins*. Buletinul Institutului Politehnic din Iaşi, Tom LVI(LX), Fasc. 2, Secţia Construcţii de Maşini, pp. 215-220, ISSN 1011-2855.

5. Zamani, N.G. (2005). *CATIA V5-FEA Tutorials*, SDC Publications, ISBN 1-58503-259-X.

Received: July 10, 2011 / Accepted: November 30, 2011 / Paper available online: December 10, 2011